

## Synthesis and Structure of $\text{Cu}_4^+ \text{Mo}_5^{6+} \text{O}_{17}^*$

E. M. McCARRON III AND J. C. CALABRESE

*Central Research and Development Department,  
E.I. du Pont de Nemours and Company, Experimental Station,  
Wilmington, Delaware 19898*

Received November 27, 1985; in revised form February 6, 1986

Crystals of  $\text{Cu}_4^+ \text{Mo}_5^{6+} \text{O}_{17}$  have been grown both hydrothermally and by the Bridgman technique from stoichiometric mixtures of the binary oxides.  $\text{Cu}_4 \text{Mo}_5 \text{O}_{17}$  crystallizes in space group *PI* with cell parameters  $a = 9.573(2)$ ,  $b = 10.958(2)$ ,  $c = 6.782(2)$  Å,  $\alpha = 91.63(2)$ ,  $\beta = 111.01(2)$ ,  $\lambda = 72.96(1)^\circ$ , and  $V = 632.60$  Å<sup>3</sup> ( $Z = 2$ ). The structure was solved by the Patterson method and refined to  $R = 0.026$  using 2223 independent reflections. The structure can be described as consisting in part of infinite, stepped ribbons of edge-sharing molybdenum oxide octahedra with a 2,3  $\circ$  3,2 cluster repeat pattern. These molybdenum oxide ribbons propagate along the  $a$  axis and are joined together by copper oxide "hooks" to complete a three dimensional network. The "hooks" are formed by a linking of the four independent copper oxide polyhedra: three tetrahedra and one pseudo-octahedron (in fact, a linear coordination of the copper with two short *trans* ( $\sim 1.9$  Å) and four long ( $> 2.3$  Å) oxygen interactions). The five independent molybdenum octahedra all show distortions typical of Mo(VI) oxides. A similarity in the lattice parameters of  $\text{Cu}_4 \text{Mo}_5 \text{O}_{17}$  and  $\text{Li}_4 \text{Mo}_5 \text{O}_{17}$  is noted. The electronic and catalytic properties of  $\text{Cu}_4 \text{Mo}_5 \text{O}_{17}$  are also reported. © 1986 Academic Press, Inc.

### Introduction

In our earlier publication on the structure of  $\text{Cu}_6 \text{Mo}_5 \text{O}_{18}$  (1), the general difficulties encountered in attempts at solid state synthesis within the  $\text{Cu}_2\text{O}-\text{CuO}-\text{MoO}_3$  system were discussed. In particular, poor control of the oxygen partial pressure during reaction appears to have been responsible for a number of inconsistent reports concerning the nature of the Cu/Mo/O phase diagram (2-4).

Clarification of the subsolidus phase diagram for the Cu/Mo/O system must rely on single-crystal growth and subsequent structure determination. In the cupric molyb-

date system, the structures of  $\text{CuMoO}_4$  (5) and  $\text{Cu}_3 \text{Mo}_2 \text{O}_9$  (6) have been determined. In addition, the structure of a mixed cupric-cuprous molybdate,  $\text{Cu}_{4-x} \text{Mo}_3 \text{O}_{12}$  ( $x \sim 0.15$ ) (7), has also been reported. We have concentrated our synthetic efforts on the formation of cuprous molybdates. Recently, we reported on the hydrothermal synthesis and crystal structure of  $\text{Cu}_6^+ \text{Mo}_5^{6+} \text{O}_{18}$  (1). We now report on the preparation and crystal structure of the new cuprous molybdate,  $\text{Cu}_4^+ \text{Mo}_5^{6+} \text{O}_{17}$ .

### Experimental

*Hydrothermal synthesis.* The stoichiometric quantities of  $\text{Cu}_2\text{O}$  and  $\text{MoO}_3$  necessary to make a 5-g sample of  $\text{Cu}_4 \text{Mo}_5 \text{O}_{17}$

\* Contribution No. 3949.

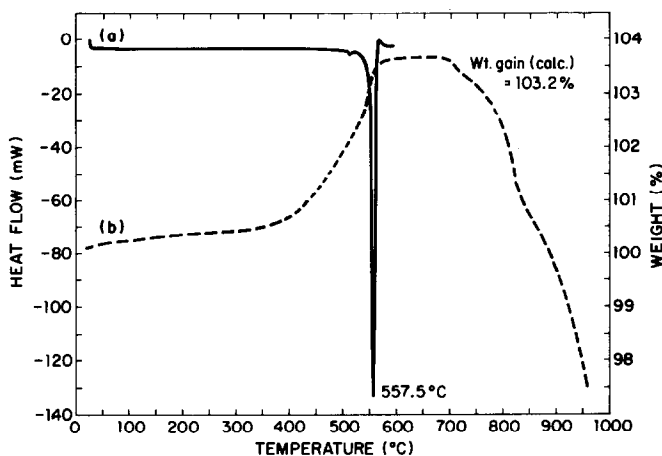


FIG. 1. Thermal analysis curves for  $\text{Cu}_4\text{Mo}_5\text{O}_{17}$ : (a) DSC in nitrogen and (b) TGA in oxygen (heating rates  $5^\circ\text{C}/\text{min}$ ). The observed TGA weight gain of  $\sim 3.5\%$  is in good agreement with the oxygen uptake calculated for  $\text{Cu}^{1+} \rightarrow \text{Cu}^{2+}$  (3.2%).

were sealed into gold tubes ( $\frac{3}{8}$ -in. diam, 6 in. long) along with 5 ml distilled water. The tubes were then sealed in air. The sealed tubes were subjected to 3 kbar pressure in an autoclave and subsequently heated to  $500^\circ\text{C}$  for 12 hr. The autoclave was slow-cooled at  $10^\circ\text{C}/\text{hr}$  to room temperature. Upon opening, the tubes contained beautifully faceted, dark metallic-looking crystals of millimeter dimensions. The crystals were water-washed and air-dried. Under the microscope, very thin crystals appeared reddish-brown in transmitted light. A suitable single crystal was chosen for the structure determination.

**Bridgman growth.** For measurements of the electrical properties of  $\text{Cu}_4\text{Mo}_5\text{O}_{17}$ , crystals larger than those grown hydrothermally were desired. Since  $\text{Cu}_4\text{Mo}_5\text{O}_{17}$  melts congruently (see Fig. 1), the standard Bridgman technique was applied (8). Boules 1 cm in diameter were grown from which crystals, several millimeters on an edge, could be cleaved.

**Analysis.** The chemical composition of single crystals of  $\text{Cu}_4\text{Mo}_5\text{O}_{17}$  was checked both by conventional chemical analysis and electron microprobe. The results were as

follows: standard chemical analysis<sup>1</sup>—Cu = 24.7(4)%, Mo = 46.8(3)%, O = 28.1(4)%; microprobe analysis—Cu = 23.6(1.2)%, Mo = 47.7(2.4)%; calculated for  $\text{Cu}_4\text{Mo}_5\text{O}_{17}$ —Cu = 25.27%, Mo = 47.69%, O = 27.04%.

**Thermal analysis.** Thermogravimetric analysis was carried out on a Dupont 951-1090B instrument at a heating rate of  $5^\circ\text{C}/\text{min}$  in an oxygen atmosphere. Differential scanning calorimetry was performed with a Du Pont 910-1090B instrument at a heating rate of  $5^\circ\text{C}/\text{min}$  in a nitrogen atmosphere. The traces are displayed in Fig. 1.

**Electrical measurements.** Resistivity measurements were made on single crystals of  $\text{Cu}_4\text{Mo}_5\text{O}_{17}$  utilizing the standard 4-probe technique. Indium contacts were soldered onto the crystals in a nitrogen atmosphere to avoid oxidation. The data are plotted in Fig. 2.

**X-ray powder diffraction.** X-ray powder diffraction patterns were obtained with a Guinier-Hägg type focusing camera ( $r = 40$

<sup>1</sup> Metals were determined by atomic absorption spectroscopy and oxygen was determined by oxygen fusion in an inductively coupled carbon crucible under argon.

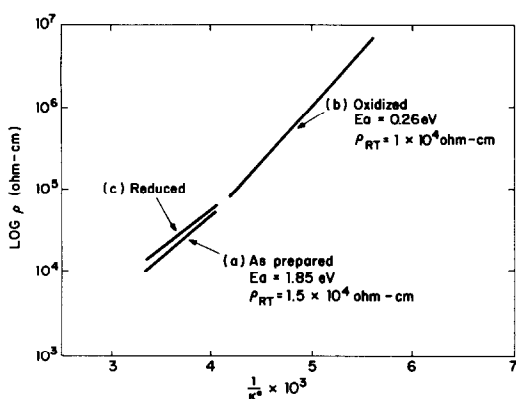


FIG. 2. A plot of the resistivity data for  $\text{Cu}_4\text{Mo}_5\text{O}_{17}$ .

mm). The radiation used was monochromatic  $\text{CuK}\alpha_1$  and the internal standard was silicon. An Optronics P-1700 photomation instrument was used to collect absorbance data from the film. Peak positions and relative intensities were determined with local computer programs. The lattice parameters were refined by a least-squares procedure. The refined triclinic lattice parameters for  $\text{Cu}_4\text{Mo}_5\text{O}_{17}$  are  $a = 9.573(2)$ ,  $b = 10.958(2)$ ,  $c = 6.782(2)$  Å,  $\alpha = 91.63(2)$ ,  $\beta = 111.01(2)$ ,  $\gamma = 72.96(1)^\circ$ , and  $V = 632.60$  Å<sup>3</sup>; with figures of merit  $F_{20} = 58$  (9) and  $M_{20} = 34$  (10).

The X-ray powder diffraction data for  $\text{Cu}_4\text{Mo}_5\text{O}_{17}$  is given in Table I along with the  $II_0$  calculated on the basis of the single crystal results. Also compared in Table I are the unit cell parameters for  $\text{Cu}_4\text{Mo}_5\text{O}_{17}$  and  $\text{Li}_4\text{Mo}_5\text{O}_{17}$  (11).

**Structural determination.** Data were collected with an Enraf-Nonius CAD4 X-ray diffractometer (equipped with a monochromatic  $\text{MoK}\alpha$  source) using a parallelepiped crystal of  $\text{Cu}_4\text{Mo}_5\text{O}_{17}$  with the dimensions,  $0.055 \times 0.055 \times 0.150$  mm. Twenty-five diffraction maxima were located and used to obtain the cell parameters;  $a = 9.570(2)$ ,  $b = 10.959(5)$ ,  $c = 6.788(2)$  Å,  $\alpha = 91.68(3)$ ,  $\beta = 111.00(2)$ ,  $\gamma = 72.97(3)^\circ$ . For  $Z = 2$ , the calculated density is  $5.275$  g/cm<sup>3</sup>.

A total of 2240 reflections were collected at ambient temperature using the  $\omega$ -scan

mode in the range,  $4^\circ < 2\theta < 50^\circ$ , with a  $(0.8 + 0.35 \tan \theta)$  scan range at  $2^\circ/\text{min}$ . There was no evidence of radiation damage to the crystal during data collection. The data were treated in the usual fashion for Lorentz-polarization and absorption (12), yielding 2223 independent reflections with  $I \geq 3\sigma$ . With  $\mu = 113.79$  cm<sup>-1</sup>, the transmission factors varied from 0.24 to 0.61.

The structure was solved using an automated Patterson solution method and re-

TABLE I  
THE POWDER PATTERN OF  $\text{Cu}_4\text{Mo}_5\text{O}_{17}$  AND A  
COMPARISON OF THE UNIT CELL PARAMETERS OF  
 $\text{Cu}_4\text{Mo}_5\text{O}_{17}$  AND  $\text{Li}_4\text{Mo}_5\text{O}_{17}$

$II_0(\text{calc})$	$II_0$	$h$	$k$	$l$	$d(\text{obs})\text{Å}$	$d(\text{calc})\text{Å}$	$2\theta(\text{obs})^\circ$
<0.5	2	1	1	0	7.8420	7.8696	11.272
19	18	0	0	1	6.2974	6.3076	14.051
34	41	0	1	1	5.6146	5.6162	15.770
4	8	0	1	-1	5.2053	5.2042	16.589
3		1	2	0		5.2084	
<0.5		0	2	0		5.2189	
8	16	2	1	-1	4.4177	4.4217	17.019
5	10	1	0	1	4.3574	4.3615	20.082
13	22	2	0	-1	4.3401	4.3438	20.363
3	3	1	2	-1	4.3191	4.3206	20.445
1	3	0	2	1	4.2022	4.2021	20.546
40	56	-1	2	0	3.9458	3.9483	21.124
17	18	-1	1	-1	3.7473	3.7483	22.514
2	3	-2	1	1	3.6957	3.6958	23.723
47	56	1	3	0	3.6280	3.6289	24.059
2	4	-2	1	0	3.5812	3.5811	24.515
6	12	0	3	0	3.4788	3.4792	24.841
3	4	1	0	-2	3.3900	3.3896	25.584
59	49	1	3	-1	3.2393	3.2401	26.266
4	3	-1	1	2	3.1971	3.1974	27.512
7	3	3	1	-1	3.1675	3.1682	27.882
<0.5		0	3	1		3.1636	
100	100	2	0	-2	3.1451	3.1448	28.148
5	4	0	1	2	3.0969	3.0935	28.352
32	47	-1	2	-1	3.0413	3.0409	28.803
7	8	3	2	-1	3.0254	3.0246	29.342
2	72	-2	2	1	2.9913	2.9910	29.500
94		2	2	1		2.9908	
6	7	0	1	-2	2.9498	2.9497	29.844
4	4	0	3	-1	2.9435	2.9416	30.273
13	19	-1	3	0	2.9240	2.9252	30.339
24	28	-2	1	2	2.9032	2.9023	30.546
5	18	-2	2	0	2.8978	2.8969	30.771
33	56	-1	3	1	2.8807	2.8805	30.831
28		1	2	-2		2.8802	
<0.5		2	2	-2		2.8750	
<0.5		3	2	0		2.8880	

Unit cell constants for $\text{A}_4\text{Mo}_5\text{O}_{17}$ (A = Cu, Li <sup>2+</sup> )							
	$a(\text{Å})$	$b(\text{Å})$	$c(\text{Å})$	$\alpha$	$\beta$	$\gamma$	$V(\text{Å}^3)$
$\text{Cu}_4\text{Mo}_5\text{O}_{17}$	9.573	10.958	6.782	91.63°	111.01°	72.96°	632.6
$\text{Li}_4\text{Mo}_5\text{O}_{17}$	9.481	10.812	6.786	91.20°	110.20°	72.98°	621.8

TABLE II  
THE ATOMIC COORDINATES ( $\times 10,000$ ) AND THE  
ISOTROPIC THERMAL PARAMETERS FOR  $\text{Cu}_4\text{Mo}_5\text{O}_{17}$

Atom	X	Y	Z	$B_{\text{eq}}(\text{\AA}^2)^a$
Mo(1)	5574.2(6)	6,720.5(5)	3499.7(8)	0.6(1)'
Mo(2)	3768.8(5)	10,272.0(5)	1338.8(8)	0.5(1)'
Mo(3)	2086.6(5)	8,003.9(5)	-170.3(8)	0.5(1)'
Mo(4)	393.3(5)	11,486.2(5)	-2422.5(8)	0.6(1)'
Mo(5)	8105.7(6)	6,123.9(5)	1276.2(8)	0.6(1)'
Cu(1)	7777.5(9)	4,441.3(8)	6979.0(14)	1.8(1)'
Cu(2)	7096.9(9)	10,790.7(10)	4552.0(14)	2.4(1)'
Cu(3)	9006.2(10)	7,053.8(10)	6865.8(14)	2.0(1)'
Cu(4)	5422.3(10)	3,805.0(10)	2262.0(14)	2.0(1)'
O(1)	3288(5)	6,545(4)	1642(7)	0.9(1)'
O(2)	4995(5)	7,327(4)	5576(7)	1.2(1)'
O(3)	-44(5)	13,260(4)	-2732(7)	0.8(1)'
O(4)	4176(5)	8,449(4)	1599(7)	0.7(1)'
O(5)	8312(5)	5,875(4)	-1192(8)	1.2(1)'
O(6)	2502(5)	11,781(4)	-515(7)	0.7(1)'
O(7)	6149(5)	5,030(4)	4109(7)	1.0(1)'
O(8)	2478(5)	7,653(5)	-2455(8)	1.3(1)'
O(9)	3391(5)	10,656(4)	3591(8)	1.1(1)'
O(10)	5691(5)	10,363(4)	1898(7)	0.9(1)'
O(11)	7480(5)	6,969(4)	4075(7)	1.0(1)'
O(12)	135(5)	7,940(4)	-811(7)	0.9(1)'
O(13)	1645(5)	9,889(4)	-523(7)	0.7(1)'
O(14)	9005(5)	4,641(4)	2662(7)	1.1(1)'
O(15)	5997(5)	6,319(4)	552(7)	0.8(1)'
O(16)	-1499(5)	11,317(4)	-2915(7)	0.9(1)'
O(17)	814(5)	11,002(5)	-4605(8)	1.3(1)'

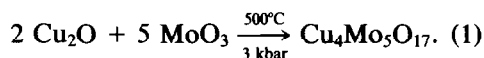
$$^a B_{\text{eq}} = \frac{4}{3} \sum_i \sum_j \beta_{ij} a_i \cdot a_j.$$

fined in space group  $P\bar{1}$  with full-matrix least squares to  $R = 0.026$  and  $R_w = 0.039$ , where  $R_w = [\sum w(|F_o| - |F_c|)^2 / \sum w|F_o|^2]^{1/2}$  with  $w$  proportional to  $[\sigma^2(I) + (0.03I)^2]^{-1/2}$ . The refinement also included a term for isotropic extinction which resulted in  $g = 0.19(1) \times 10^{-4}$  mm. The final esd of an observation of unit weight is 1.10. The largest final difference-Fourier map residual was  $0.97 \text{ e/\AA}^3$ . The final positional parameters are listed in Table II, and bond lengths in Table III.<sup>2</sup>

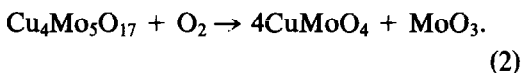
<sup>2</sup> See NAPS Document No. 04386 for 8 pages of supplementary materials from ASIS/NAPS, Microfiche Publications, P.O. Box 3513, Grand Central Station, New York, N.Y. 10163. Remit in advance \$4.00 for microfiche copy or for photocopy, \$7.75 up to 20 pages plus \$.30 for each additional page. All orders must be prepaid.

## Results and Discussion

Analogous to the synthesis of  $\text{Cu}_6\text{Mo}_5\text{O}_{18}$  (1),  $\text{Cu}_4\text{Mo}_5\text{O}_{17}$  was prepared hydrothermally at  $500^\circ\text{C}$  and 3 kbar pressure from a stoichiometric mix of the simple binary oxides:



Subsequently, it was observed that  $\text{Cu}_4\text{Mo}_5\text{O}_{17}$  formed a congruent melt (Fig. 1, DSC curve) and therefore larger single crystals, suitable for use in making the resistivity measurements, could be prepared via the Bridgman technique. The stoichiometry of  $\text{Cu}_4\text{Mo}_5\text{O}_{17}$  was checked by oxygen uptake (Fig. 1, TGA curve) and found to be consistent with the conversion of  $\text{Cu}^{1+}$  to  $\text{Cu}^{2+}$  according to



As in the case of  $\text{Cu}_6\text{Mo}_5\text{O}_{18}$ , both ESCA<sup>3</sup> and ESR<sup>4</sup> measurements performed on freshly prepared samples handled under nitrogen confirmed the oxidation state assignments as  $\text{Cu}_4^{1+}\text{Mo}_5^{6+}\text{O}_{17}$ .

The 4-probe electrical resistivity measurements are also concordant with the oxidation state assignments made above. Freshly prepared  $\text{Cu}_4\text{Mo}_5\text{O}_{17}$  is a semicon-

<sup>3</sup> ESCA spectra were recorded on a Du Pont 650 instrument. Freshly prepared  $\text{Cu}_4\text{Mo}_5\text{O}_{17}$  samples handled under nitrogen give a single Cu  $2p_{3/2}$   $E_B$  line at 932.6 eV, indicative of  $\text{Cu}^{1+}$ . As the samples aged in oxygen a second line appeared at 935.5 eV, indicative of  $\text{Cu}^{2+}$ ; for  $\text{CuMoO}_4$ , Cu  $2p_{3/2}$   $E_B = 935.4$  eV. For a discussion of the ESCA results see J. Haber, T. Machej, L. Ungier, and J. Ziółkowski, *J. Solid State Chem.* **25**, 207 (1978).

<sup>4</sup> ESR spectra were recorded on a Bruker ER-420 instrument. The lack of a detectable  $\text{Cu}^{2+}$  signal on freshly prepared  $\text{Cu}_6\text{Mo}_5\text{O}_{18}$  samples handled under nitrogen implies that copper is present in the  $\text{Cu}^{1+}$  oxidation state.  $\text{Cu}_6\text{Mo}_5\text{O}_{18}$  samples aged in oxygen did exhibit a  $\text{Cu}^{2+}$  signal at liquid nitrogen temperature. No attempt was made to quantify the amount of  $\text{Cu}^{2+}$  present.

TABLE III  
 BOND LENGTHS (IN Å) FOR  $\text{Cu}_4\text{Mo}_5\text{O}_{17}$ 

Mo(1)–O(1)	2.161(4)	Mo(2)–O(4)	1.921(4)	Mo(3)–O(1)	1.849(4)
–O(2)	1.739(5)	–O(6)	1.909(4)	–O(4)	2.120(4)
–O(4)	2.113(4)	–O(9)	1.707(5)	–O(8)	1.729(5)
–O(7)	1.787(4)	–O(10) <sup>f</sup>	2.468(5)	–O(12)	1.782(4)
–O(11)	1.824(4)	–O(10)	1.773(4)	–O(13)	1.988(4)
–O(15)	2.188(4)	–O(13)	2.129(4)	–O(16)	2.401(5)
Mo(4)–O(3)	1.867(4)	Mo(5)–O(3)	2.063(4)		
–O(6)	2.083(4)	–O(5)	1.760(5)		
–O(12)	2.449(5)	–O(6)	2.224(4)		
–O(13)	1.989(4)	–O(11)	2.284(5)		
–O(16)	1.785(4)	–O(14)	1.719(4)		
–O(17)	1.702(5)	–O(15)	1.845(4)		
Cu(1)–O(1)	2.115(4)	Cu(2)–O(2)	2.395(5)	Cu(3)–O(5)	2.254(5)
–O(3)	2.049(4)	–O(8)	2.463(5)	–O(11)	1.954(5)
–O(5)	2.043(5)	–O(9)	2.301(5)	–O(12)	1.975(5)
–O(7)	1.988(5)	–O(10)	1.964(5)	–O(14)	2.168(5)
		–O(16)	1.958(5)	[–O(17)	2.742(5)]
		–O(17)	2.348(5)	[–O(9)	2.797(5)]
Cu(4)–O(2)	2.161(4)				
–O(7)	1.918(5)				
–O(8)	2.133(5)				
–O(15)	1.935(4)				

ductor with a room temperature resistivity of  $1.5 \times 10^4 \Omega\text{-cm}$  and an activation energy of  $\sim 1.85 \text{ eV}$  (Fig. 2). This activation energy, if it is a true measure of the band gap, is consistent with the reddish color of  $\text{Cu}_4\text{Mo}_5\text{O}_{17}$ . However, both the resistivity and the activation energy of  $\text{Cu}_4\text{Mo}_5\text{O}_{17}$  were observed to decrease upon either prolonged contact with oxygen or gentle heating in air (Fig. 2). These observations suggest that  $\text{Cu}^{2+}$  states, which would account for the observed extrinsic behavior, are being introduced into the band gap via oxidation. Though not quantified, ESR experiments performed on oxygen-aged samples at liquid nitrogen temperatures clearly reveal the presence of  $\text{Cu}^{2+}$  states.<sup>4</sup> Conversely, gentle heating in a hydrogen atmosphere eliminates the  $\text{Cu}^{2+}$  ESR signal and essentially restores the resistivity and activation energy to their initial values (Fig. 2).

The compounds  $\text{Cu}_4\text{Mo}_5\text{O}_{17}$  and the re-

lated  $\text{Cu}_6\text{Mo}_5\text{O}_{18}$  were tested as selective oxidation catalysts for the conversion of methanol or formaldehyde. One type of commercial catalyst for this process consists of a mixture of ferric molybdate and molybdenum trioxide (13). Previous work in our laboratory (14) has shown that, in general, molybdates are good selective oxidation catalysts owing, in part, to the favorable redox chemistry associated with  $\text{Mo}^{6+}$ . Therefore, the cuprous molybdates appeared to be interesting materials for study since, in addition to the molybdenum redox chemistry, there also existed the possibility of involving a second redox couple, namely,  $\text{Cu}^{1+} \leftrightarrow \text{Cu}^{2+} + e^-$ , in the catalytic reaction. However, under reactor conditions ( $350^\circ\text{C}$ , 7.8%  $\text{CH}_3\text{OH}$  in air) the cuprous molybdates are converted to cupric molybdate,  $\text{CuMoO}_4$ , and found to be two orders of magnitude less active than  $\text{Fe}_2\text{Mo}_3\text{O}_{12}$ . Moreover, given the conversion

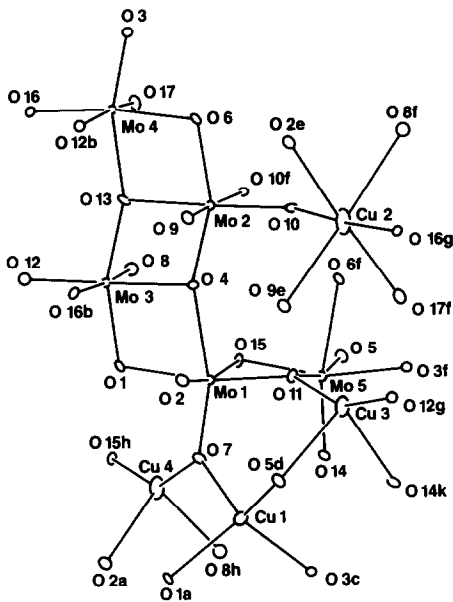


FIG. 3. The metal atoms of the asymmetric unit of  $\text{Cu}_4\text{Mo}_5\text{O}_{17}$  shown with full oxygen coordination.

to  $\text{CuMoO}_4$ , it is not surprising that  $\text{Cu}_4\text{Mo}_5\text{O}_{17}$  samples were found to be more active than  $\text{Cu}_6\text{Mo}_5\text{O}_{18}$  samples by a factor of 5–6. This result reflects the formation of an active second phase,  $\text{MoO}_3$  (Eq. (2)), in the case of copper-poor  $\text{Cu}_4\text{Mo}_5\text{O}_{17}$ , as op-

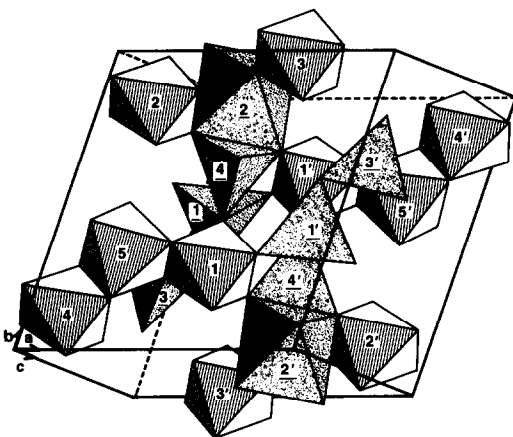


FIG. 4. The unit cell of  $\text{Cu}_4\text{Mo}_5\text{O}_{17}$  (Cu atoms, underlined; Cu polyhedra, dappled; Mo polyhedra, lined; primes indicate an inversion center at  $(\frac{1}{2}, \frac{1}{2}, \frac{1}{2})$ ).

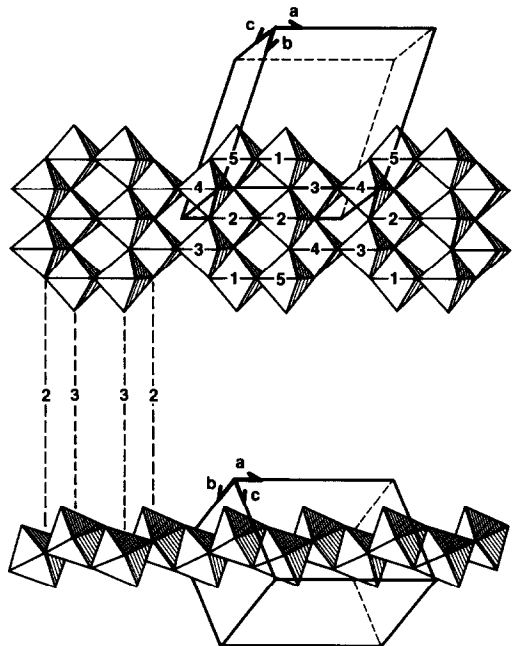
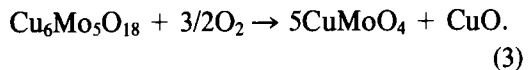


FIG. 5. Detail of the molybdenum oxide chain (shown at right angles) showing the 2,3-3,2 cluster repeat unit of the  $\text{MoO}_6$  octahedra (inversion center at  $(\frac{1}{2}, 0, 0)$ ).

posed to the formation of a relatively inactive phase,  $\text{CuO}$ , for copper-rich  $\text{Cu}_6\text{Mo}_5\text{O}_{18}$ :



Preparatory to a discussion of the structure of  $\text{Cu}_4\text{Mo}_5\text{O}_{17}$ , Fig. 3 identifies the metal atoms of the asymmetric unit and shows their full oxygen coordination. Tables III and IV list bond distances. The molybdenum atoms are all octahedrally coordinated and all show distortions typical of molybdenum(VI) oxides.<sup>5</sup> On the other hand, only one of the four copper atoms,

<sup>5</sup> For a discussion octahedral distortions in molybdenum(VI) oxides see Ref. (2) and also J. B. Goodenough, "Proceedings of the Climax 4th International Conf. on the Chem. and Uses of Molybdenum (H. F. Barry and P. C. H. Mitchell, Eds.), pp. 1–22, Climax Molybdenum Co., Ann Arbor, MI, 1982.

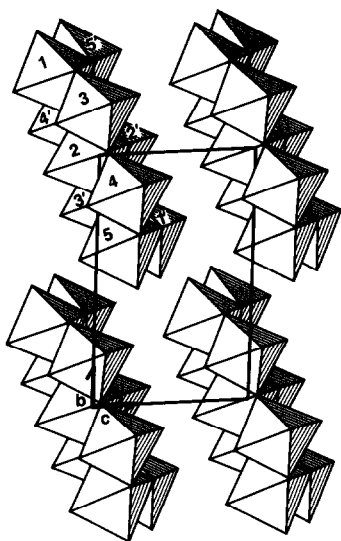


FIG. 6. The arrangement of the molybdenum oxide chains looking along the  $a$  axis.

$\text{Cu}(2)$ , has the linear (pseudo-octahedral) coordination typical of copper(I) oxides (15). The remaining three Cu atoms are tetrahedrally coordinated. Tetrahedral coordination of copper in oxides is known in two other cases,  $\text{CuNb}_3\text{O}_8$  (16) and  $\text{Cu}_6\text{Mo}_5\text{O}_{18}$  (1), only. Figure 4 shows the coordination polyhedra of the metal atoms contained within the unit cell of  $\text{Cu}_4\text{Mo}_5\text{O}_{17}$ .

The structure of  $\text{Cu}_4\text{Mo}_5\text{O}_{17}$  can best be visualized as consisting, in part, of infinite, stepped molybdenum oxide chains,  $[\text{Mo}_5\text{O}_{25/3}\text{O}_{5/2}]_n$ , which propagate along the  $a$  axis. These infinite Mo–O chains are then joined together by copper oxide “hooks”  $n[\text{Cu}_4\text{O}_{14/3}\text{O}_{3/2}]$ , to complete a three-dimensional network. The structural components of  $\text{Cu}_4\text{Mo}_5\text{O}_{17}$  and the full structure itself are shown in Figs. 5–8.

A single chain of edge-shared molybdenum octahedra is detailed in Fig. 5. The chain contains five independent  $\text{MoO}_6$  octahedra with the inversion center at  $(\frac{1}{2}, 0, 0)$  generating a  $2,3 \circ 3,2$  repeat unit. Figure 6 shows the relationship of the chains to one another. As mentioned above, the distortions of the individual  $\text{MoO}_6$  octahedra (Table III) are representative of those typically found in molybdenum(VI) oxides.<sup>5</sup> The individual Mo–O bond lengths range from 1.702 to 2.468 Å and those found in  $\text{Cu}_6\text{Mo}_5\text{O}_{18}$ , from 1.713 to 2.239 Å (1). In the  $\text{Cu}_6\text{Mo}_5\text{O}_{18}$  structure, it was noted that the molybdenyl oxygens ( $\text{Mo}=\text{O}$ ; bond lengths  $<1.8$  Å) were coordinated only to copper atoms, reflecting the strongly acidic character of these oxygens. Of the 10 molybdenyl oxygens found in the  $\text{Cu}_4\text{Mo}_5\text{O}_{17}$  structure (see Table IV), seven are coordinated

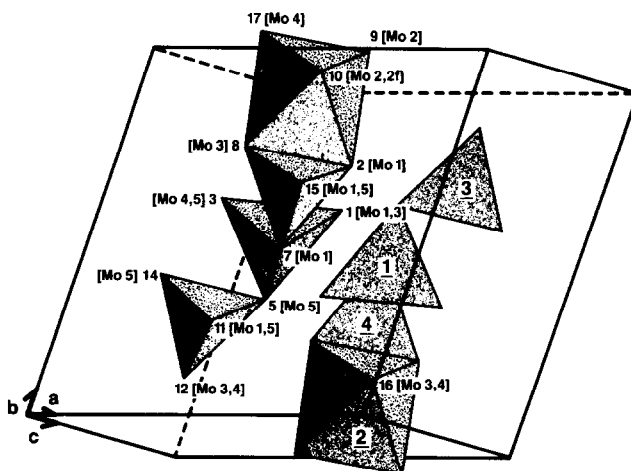


FIG. 7. Copper oxide “hooks” (Cu atoms, underlined) showing the oxygen coordination in brackets.

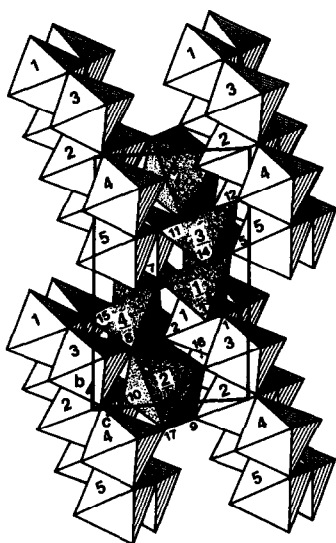


FIG. 8. The structure of  $\text{Cu}_4\text{Mo}_5\text{O}_{17}$  looking along the  $a$  axis (Cu atoms, underlined; Cu polyhedra, dappled; Mo polyhedra, lined; oxygen atoms, small numerals).

solely to copper atoms and, of the remaining three, two coordinate to both a copper atom and a molybdenum atom and one only to one other molybdenum atom. In the latter cases, the interactions of the molybdenyl oxygens with the other molybdenum atoms are very weak (bond lengths  $>2.4$  Å), indicative of the acidic nature of molybdenyl oxygens.

The copper oxides "hooks" are shown in Fig. 7. Each "hook" consists of three distorted  $\text{CuO}_4$  tetrahedra and one apparent  $\text{CuO}_6$  octahedron. At first, it appeared that the two types of copper environments might be indicative of a mixed valence situation because although tetrahedral coordination had been observed previously for  $\text{Cu}^{1+}$  ion in oxides (1, 16), octahedrally coordinated  $\text{Cu}^{1+}$  had not been reported.<sup>6</sup> One

<sup>6</sup> This is not strictly true. In both  $\text{CuNb}_3\text{O}_8$  and  $\text{Cu}_6\text{Mo}_5\text{O}_{18}$ , copper atoms are found coordinated with four short and two long *cis* bonds to oxygen. The question, as to deciding whether to describe the coordination as tetrahedral or octahedral, then becomes, at what point do the Cu–O interactions become negligible?

possible interpretation of the distorted octahedral coordination of Cu(2) might be that it was the result of a Jahn-Teller distortion involving a  $\text{Cu}^{2+}$  ion. However, a number of observations were inconsistent with this interpretation. First, for the vast majority of cupric compounds, Jahn-Teller distortions<sup>7</sup> of the octahedral bonding symmetry are of the type, 4 short and 2 *trans* long bonds. This is opposite to the distortion observed for Cu(2) (four long ( $>2.3$  Å) and two *trans* short ( $<2.0$  Å) bonds). Second, the semiconducting behavior of  $\text{Cu}_4\text{Mo}_5\text{O}_{17}$  implies that the electrons should be localized, necessitating the creation of a corresponding molybdenum(V) ion, yet, based on bond valences determined from bond strength calculations (see Table IV); all the molybdenum atoms of  $\text{Cu}_4\text{Mo}_5\text{O}_{17}$  show coordinations typical of  $\text{Mo}^{6+}$ .<sup>5</sup> Finally, no  $\text{Cu}^{2+}$  ESR signal could be detected for freshly prepared samples of  $\text{Cu}_4\text{Mo}_5\text{O}_{17}$ . Therefore, Cu(2) is most properly described as having the linear coordination typical of  $\text{Cu}^{1+}$  ion.

The formulation  $\text{Cu}_4^1+\text{Mo}_5^6+\text{O}_{17}$  is further supported by the earlier report of the formation of the Li analog,  $\text{Li}_4\text{Mo}_5\text{O}_{17}$  (11). Although the structure of  $\text{Li}_4\text{Mo}_5\text{O}_{17}$  has not been determined in detail, the similarity of the unit cell parameters (see Table I) suggests that the structure type is the same for both  $\text{Cu}_4\text{Mo}_5\text{O}_{17}$  and  $\text{Li}_4\text{Mo}_5\text{O}_{17}$ . In the related case of the niobates,  $\text{ANb}_3\text{O}_8$  ( $A = \text{Li}, \text{Cu}$ ) (17, 16), for which the crystal structures are known in detail, the substitution of copper for lithium is found to result also

<sup>7</sup> For a discussion of the stereochemistry of copper(II), see F. A. Cotton and G. Wilkinson, "Advanced Inorganic Chemistry," 4th ed., pp. 811–812, Wiley, New York, 1980, and references therein.

<sup>8</sup> The unit cell parameters presented for  $\text{Li}_4\text{Mo}_5\text{O}_{17}$  are a transformation of the lattice constants given in Ref. (1). The transformation matrix used was

$$\begin{bmatrix} 0 & \bar{1} & 0 \\ 0 & 0 & 1 \\ \bar{1} & 0 & 0 \end{bmatrix}.$$



TABLE IV  
BOND DISTANCES (IN Å) EMPHASIZING OXYGEN  
COORDINATION<sup>a</sup>

O(1)–Mo(3)	1.849	[1.11]	<sup>b</sup> O(2)–Mo(1)	1.739	[1.61]
–Mo(1)	2.161	[0.44]	–Cu(4)	2.161	
–Cu(1)	2.115		–Cu(2)	2.395	
O(3)–Mo(4)	1.867	[1.05]	O(4)–Mo(2)	1.921	[0.88]
–Mo(5)	2.063	[0.58]	–Mo(1)	2.113	[0.50]
–Cu(1)	2.049		–Mo(3)	2.120	[0.49]
<sup>b</sup> O(5)–Mo(5)	1.760	[1.50]	O(6)–Mo(2)	1.909	[0.92]
–Cu(1)	2.043		–Mo(4)	2.084	[0.54]
–Cu(3)	2.254		–Mo(5)	2.224	[0.37]
<sup>b</sup> O(7)–Mo(1)	1.787	[1.36]	<sup>b</sup> O(8)–Mo(3)	1.729	[1.66]
–Cu(4)	1.918		–Cu(4)	2.133	
–Cu(1)	1.988		–Cu(2)	2.463	
<sup>b</sup> O(9)–Mo(2)	1.707	[1.80]	<sup>b</sup> O(10)–Mo(2)	1.773	[1.43]
–Cu(2)	2.301		–Mo(2) <sup>f</sup>	2.468	[0.20]
O(11)–Mo(1)	1.824	[1.21]	<sup>b</sup> O(12)–Mo(3)	1.782	[1.39]
–Mo(5)	2.284	[0.31]	–Mo(4)	2.449	[0.21]
–Cu(3)	1.954		–Cu(3)	1.975	
O(13)–Mo(3)	1.988	[0.72]	<sup>b</sup> O(14)–Mo(5)	1.719	[1.72]
–Mo(4)	1.989	[0.72]	–Cu(3)	2.168	
–Mo(2)	2.129	[0.48]			
O(15)–Mo(5)	1.845	[1.13]	<sup>b</sup> O(16)–Mo(4)	1.785	[1.37]
–Mo(1)	2.188	[0.40]	–Mo(3)	2.401	[0.23]
–Cu(1)	1.935		–Cu(2)	1.958	
<sup>b</sup> O(17)–Mo(4)	1.702	[1.83]			
–Cu(2)	2.348				

<sup>a</sup> Mo–O bond strengths in brackets.<sup>9</sup>

<sup>b</sup> Short molybdenyl (Mo=O) type interactions (bond strength >1.33).

in the retention of the structure type, even though a change in the coordination of the A atom does occur. For  $\text{LiNb}_3\text{O}_8$ , lithium occupies a distorted octahedron with Li–O distances ranging from 2.08 to 2.34 Å. In  $\text{CuNb}_3\text{O}_8$ , the copper is at the center of a very distorted tetrahedron with Cu–O distances ranging from 2.08 to 2.25 Å; two other oxygen atoms (*cis*) are found at 2.43 and 2.49 Å from the copper, completing a distorted octahedron. The unsuitability of octahedral coordination for  $\text{Cu}^{1+}$  cations was also observed in  $\text{Cu}_6^{1+}\text{Mo}_5^{6+}\text{O}_{18}$  (I). In  $\text{Cu}_6\text{Mo}_5\text{O}_{18}$ , the three independent copper atoms are best described as being tetrahe-

drally coordinated, but one of the copper atoms also can be described as sitting in a very distorted octahedron with four short (1.91–2.17 Å) and two *cis* long (2.84 and 2.96 Å) oxygen interactions. This type of distortion is also found in the present structure, where Cu(3) has in addition to four short bonds (1.954–2.254 Å), two long *cis* oxygen interactions (2.742 (0.17 $f$ ) and 2.797 Å (0.9 $e$ ), as shown in Fig. 3). It therefore appears that the inability of a  $\text{Cu}^{1+}$  ion to stabilize octahedral coordination accounts for the distortions of the copper oxide polyhedra observed. As a result, two general types of distortion from octahedral symmetry now can be recognized: one involving the movement away of two *cis* oxygens to give a distorted tetrahedral coordination about the copper, and a second involving the moving together of two *trans* oxygens (with a consequential lengthening of the remaining four oxygen interactions) to give the linear coordination typical of copper(I) oxides.

Based on the  $\text{ANb}_3\text{O}_8$  (A = Li, Cu) observations, it can be predicted that the structure of  $\text{Li}_4\text{Mo}_5\text{O}_{17}$  will differ from that of  $\text{Cu}_4\text{Mo}_5\text{O}_{17}$  in such a way that small shifts in the  $\text{Cu}_4\text{Mo}_5\text{O}_{17}$  oxygen positions would accommodate an octahedral coordination of the lithium atoms. We are currently attempting to grow crystals of  $\text{Li}_4\text{Mo}_5\text{O}_{17}$  and to synthesize  $\text{Li}_6\text{Mo}_5\text{O}_{18}$  crystals for structure determinations. We would like to be able to make detailed structural comparisons with the corresponding copper molybdates in an attempt to gain further insight into the coordination chemistry of  $\text{Cu}^{1+}$ .

### Acknowledgments

The authors thank C. M. Foris for her help in refining the powder pattern data, P. E. Bierstedt for obtaining the ESCA results, J. L. Gillson for making the resistivity measurements, C. J. Machiels for studying the catalytic properties, and C. Dybowski for providing the ESR results. The authors also acknowledge the helpful discussions with Dr. A. W. Sleight.

<sup>9</sup> The bond strength,  $s$ , is derived from the expression,  $s = (d/1.882)^{-6.0}$ , where  $d$  is the bond length in Å. Taken from J. C. J. Bart and U. Ragaini, "Proceedings of the Climax 3rd International Conf. on the Chem. and Uses of Molybdenum" (H. F. Barry and P. C. H. Mitchell, Eds.), Climax Molybdenum Co., Ann Arbor, MI, 1979.

**References**

1. E. M. McCARRON III AND J. C. CALABRESE, *J. Solid State Chem.* **62**, 64 (1986).
2. K. NASSAU AND J. W. SHIEVER, *J. Am. Ceram. Soc.* **45**, 36 (1969).
3. T. MACHEJ AND J. ZIÓŁKOWSKI, *J. Solid State Chem.* **31**, 135 (1980).
4. T. MACHEJ AND J. ZIÓŁKOWSKI, *J. Solid State Chem.* **31**, 145 (1980).
5. S. C. ABRAHAMS, J. L. BERNSTEIN, AND P. B. JAMIESON, *J. Chem. Phys.* **48**, 2619 (1968).
6. L. KIHNBORG, R. NORRESTAM, AND B. OLIVECRONA, *Acta Crystallogr. Sect. B* **27**, 2066 (1971).
7. L. KATZ, AND KESECALLY, AND L. KIHNBORG, *Acta Crystallogr. Sect. B* **27**, 2071 (1971).
8. R. A. LAUDISE, "The Growth of Single Crystals," pp. 161-173, Prentice-Hall, Englewood Cliffs, N.J., 1970.
9. G. S. SMITH AND R. L. SNYDER, *J. Appl. Cryst.* **12**, 60 (1979).
10. P. M. DE WOLFF, *J. Appl. Cryst.* **1**, 108 (1968).
11. W. S. BROWER, H. S. PARKER, R. S. ROTH, AND J. L. WARING, *J. Cryst. Growth* **16**, 115 (1972).
12. P. COPPENS, *Acta Crystallogr.* **18**, 1035 (1965).
13. C. J. MACHIELS, U. CHOWDHRY, R. H. STALEY, F. OHUCHI, AND A. W. SLEIGHT, "Catalytic Conversions for Synthesis Gas and Alcohols to Chemicals" (R. G. Harman, Ed.), p. 413, Plenum, New York, 1984.
14. W.-H. CHENG, U. CHOWDHRY, A. FERRETTI, L. E. FIRMENT, R. P. GROFF, C. J. MACHIELS, E. M. McCARRON, F. OHUCHI, R. H. STALEY, AND A. W. SLEIGHT, "Heterogeneous Catalysis," Proceedings of the 2nd Symposium of IUCCP of the Dept. of Chemistry, Texas A&M (B. L. Sharp, Ed.), pp. 165-181, Texas A&M Univ. Press, College Station, 1984.
15. A. F. WELLS, "Structural Inorganic Chemistry," 4th ed., Clarendon Press, Oxford, 1975.
16. B-O. MARINDER, P-E. WERNER, E. WAHLSTROM, AND G. MALMROS, *Acta Chem. Scand. A* **34**, 51 (1980).
17. M. LUNDBERG, *Acta Chem. Scand.* **25**, 3337 (1971).